
Enforcing Hard Constraints with Soft Barriers: Safe Reinforcement Learning in Unknown Stochastic Environments

Anonymous Authors¹

Abstract

Reinforcement Learning (RL) has long grappled with the issue of ensuring agent safety in unpredictable and stochastic environments, particularly under hard constraints that require the system state not to reach unsafe regions. Conventional safe RL methods such as those based on the Constrained Markov Decision Process (CMDP) paradigm formulate safety violations in a cost function and try to constrain the expectation of cumulative cost under a threshold. However, it is often difficult to effectively capture and enforce hard reachability-based safety constraints indirectly with such constraints on safety violation cost. In this work, we leverage the notion of barrier function to explicitly encode the hard safety chance constraints, and as the environment is unknown, relax them to our design of *generative-model-based soft barrier functions*. Based on such soft barriers, we propose a novel safe RL approach with bi-level optimization that can jointly learn the unknown environment and optimize the control policy, while effectively avoiding the unsafe region with safety probability optimization. Experiments on a set of examples demonstrate that our approach can effectively enforce hard safety chance constraints and significantly outperform CMDP-based baseline methods in system safe rates measured via simulations.

1. Introduction

Reinforcement learning (RL) has shown promising successes in learning complex policies for games (Silver et al., 2018), robots (Zhao et al., 2020; Yang et al., 2023), and cyber-physical systems like smart buildings (Wei et al., 2017; Xu et al., 2021a; 2022), by maximizing a cumula-

tive reward objective as the optimization goal. However, real-world safety-critical applications, such as autonomous cars (Liu et al., 2022; 2023b;a), still hesitate to adopt RL policies due to safety concerns. In particular, when the environment is stochastic and unknown (Zhu et al., 2020; 2021), these applications often have *hard safety chance constraints* that require the probability of the system state not reaching certain specified unsafe regions above a threshold, e.g., autonomous cars not deviating into adjacent lanes or UAVs not colliding with trees. It is very challenging to learn a policy via RL that can meet such hard safety chance constraints.

In the literature, the Constrained Markov Decision Process (CMDP) (Altman, 1999) is a popular paradigm for addressing RL safety. Common CMDP-based methods encode safety constraints through a cost function of safety violations, and reduce the policy search space to where the expectation of cumulative discounted cost is less than a threshold. Various RL algorithms are proposed to adaptively solve CMDP through the primal-dual approach for the Lagrangian problem of CMDP. However, it is often hard for CMDP-based methods to enforce reachability-based hard safety chance constraints (i.e., the probability bound of the system state not reaching unsafe regions) with the *indirect* constraints on the expectation of cumulative cost. In particular, while reachability-based safety constraints are defined on the system state at the time point level (i.e., each point on the trajectory), the CMDP constraints only enforce the cumulative behavior in expectation at the trajectory level. In other words, the cost penalty on the system visiting the unsafe regions at a certain time point may be offset by the low cost at other times. There is a recent CMDP approach addressing hard safety constraints by using the indicator function for encoding failure probability (Wagner et al., 2021), but it requires a safe backup policy for intervention, which is difficult to achieve in unknown environments. Safe exploration with hard safety constraints has also been studied in (Wachi et al., 2018; Turchetta et al., 2016; Moldovan & Abbeel, 2012). However, these works focus on discrete state and action spaces where the hard safety constraints are defined as a set of unsafe state-action pairs that should not be visited, different from the continuous control setting we are considering.

¹Anonymous Institution, Anonymous City, Anonymous Region, Anonymous Country. Correspondence to: Anonymous Author <anon.email@domain.com>.

Preliminary work. Under review by the International Conference on Machine Learning (ICML). Do not distribute.

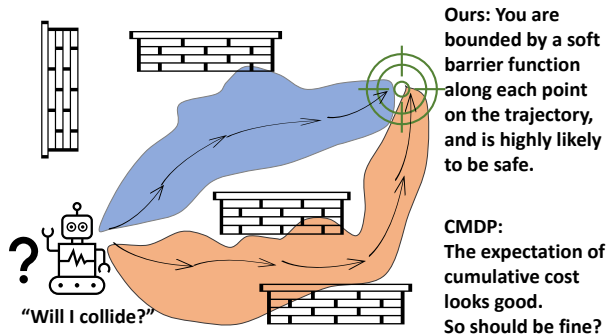


Figure 1: An RL-based robot navigation example that shows the conceptual difference between our approach and CMDP-based ones in encoding the hard safety chance constraints. The satisfaction of CMDP cannot provide any safety probability for the learned policy with any initial state, while our approach can bound/optimize the entire trajectory with a safety probability by the soft barrier function.

On the other hand, current control-theoretical approaches for model-based safe RL often try to leverage formal methods to handle hard safety constraints, e.g., by establishing safety guarantees through barrier functions or control barrier functions (Luo & Ma, 2021), or by shielding mechanisms based on reachability analysis (Huang et al., 2019; Fan et al., 2020; Huang et al., 2022) to check whether the system may enter the unsafe regions within a time horizon (Bastani et al., 2021; Huang et al., 2020; Wang et al., 2020; 2021a;b;c; 2022). However, these approaches either require explicit known system models for barrier or shielding construction or an initial safe policy to generate safe trajectory data in a deterministic environment. They cannot be applied to the unknown stochastic environments we are addressing.

To overcome the above challenges, we propose a safe RL framework by encoding the hard safety chance constraints via the learning of a *generative-model-based soft barrier function*. Specifically, we formulate and solve a novel bi-level optimization problem to learn the policy with **joint soft barrier function learning, generative modeling, and policy optimization**. The soft barrier function provides guidance for avoiding unsafe regions based on safety probability analysis and optimization. The generative model accesses the trajectory data from the environment-policy closed-loop system with stochastic differential equation (SDE) representation to learn the dynamics and stochasticity of the environment. And we further optimize the policy by maximizing the total discounted reward of the sampled synthetic trajectories from the generative model. This joint training framework is fully differentiable and can be efficiently solved via the gradients. Compared to CMDP-based methods, our approach more directly encodes the hard safety chance constraints along each point of the agent

trajectory through the soft barrier function, as shown in Figure 1. While given the unknown stochastic environment, our approach cannot provide a hard barrier and hence no deterministic safety guarantee, experimental results demonstrate that in simulations, ours can significantly outperform the CMDP-based baselines in system safe rate.

The paper is organized as follows. Section 2 introduces related works, Section 3 presents our approach, including the bi-level optimization formulation, our safe RL algorithm with generative modeling, soft barrier function learning, and policy optimization to solve the formulation and theoretical analysis of safety probability. Section 4 shows the experiments and Section 5 concludes the paper.

2. Related work

Safe RL by CMDP: CMDP-based methods encode the safety violation as a cost function and set constraints on the expectation of cumulative discounted total cost (Yang et al., 2021; Bharadhwaj et al.). The primal-dual approaches have been widely adopted to solve the Lagrangian problem of constrained policy optimization (Bai et al., 2022), such as PDO (Chow et al., 2017), OPDOP (Ding et al., 2021), CPPO (Stooke et al., 2020), FOCOPS (Zhang et al., 2020), CRPO (Xu et al., 2021b), and P3O (Shen et al., 2022). Other works leverage a world model learning (As et al., 2021) or the Lyapunov function to solve the CMDP (Chow et al., 2018), or add a safety layer for the safety constraint (Dalal et al., 2018). However, the constraints in CMDP cannot directly encode the hard time-point-level chance constraint, which hinders its application to many safety-critical systems. A recent CMDP-based work uses the indicator function for encoding failure probability as hard safety chance constraints, but it requires a safe backup policy for intervention (Wagener et al., 2021).

Model-based Safe RL by Formal Methods: Formal analysis and verification techniques have been proposed in model-based safe RL to enforce the system not to reach unsafe regions. Some works develop shielding mechanisms with a backup policy based on reachability analysis (Shao et al., 2021; Bastani et al., 2021). Other works adopt (control) barrier functions or (control) Lyapunov functions for provable safety (Emam et al., 2021; Choi et al., 2020; Cheng et al., 2019; Wang et al., 2023; Ma et al., 2021; Luo & Ma, 2021; Berkenkamp et al., 2017; Taylor et al., 2020). Moreover, recent work (Yu et al., 2022) adopts reachability analysis with CMDP to compute safe feasible sets. However, these methods either require known dynamics, assume a deterministic environment, a safe initial/backup policy, or human intervention, and thus do not apply to our setting.

Barrier Function for Safety: Barrier function is introduced as a safety certificate afflicted to the control policy for

deterministic and stochastic systems (Prajna & Jadbabaie, 2004; Prajna et al., 2004). In classical control, finding a barrier function is time-consuming and requires a lot of manual effort, where a common idea is to relax the conditions of the barrier function into optimization formulations such as linear programming (Yang et al., 2016), quadratic programming (Ames et al., 2016), and sum-of-square programming (Wang et al., 2023). However, these optimization-based approaches can hardly scale to high-dimensional systems. To this end, recent works have shown great promise in jointly training barrier function and safe policy by neural network representation for better scalability (Qin et al., 2021). Our approach leverages the paradigm of barrier function but develops the concept of a soft barrier to address unknown stochastic environments.

RL with Generative Model: Previous works of generative-model-based RL mainly focus on sample efficiency and policy optimization for the total expected return (Agarwal et al., 2020b; Li et al., 2020a; Tirinzoni et al., 2020). Some works (HasanzadeZonuzi et al., 2021; Maeda et al., 2021) address safe RL by CMDP with a generative model but only solve the tabular discrete state and action space. Besides policy optimization, the generative model in our framework also plays an important role in building a soft barrier function to facilitate the probabilistic safety analysis and optimization.

3. Our Approach

In this section, we present our framework for safe RL in an unknown stochastic environment that enforces hard safety chance constraints with soft barrier functions. In Section 3.1, we present our bi-level optimization formulation for the problem, which maximizes a total expected return while trying to avoid unsafe regions by optimizing safety probability. Specifically, we encode the hard safety chance constraints with a novel generative-model-based soft barrier function in the lower problem and maximize the performance of the policy with generative model learning in the upper problem. We then present our safe RL algorithm to solve the bi-level optimization formulation, by jointly learning the generative model (Section 3.2), soft barrier function (Section 3.3), and policy optimization (Section 3.4) via first-order gradient, as shown in Figure 2. We conduct theoretical analysis for the safety probability of the learned policy in Section 3.5.

3.1. Bilevel Optimization Problem Formulation for Safe RL with Soft Barrier

We assume that the environment can be abstracted as a finite-horizon continuous MDP $\mathcal{M}_\theta \sim (\mathcal{S}, \mathcal{A}, \mathcal{P}, r, \gamma)$, where $\mathcal{S} \subset \mathbb{R}^n$ represents the continuous state space, $\mathcal{A} \subset \mathbb{R}^m$ indicates the continuous action space, and the function class $\mathcal{P} : \mathcal{S} \times \mathcal{A} \times \mathcal{S} \rightarrow [0, 1]$ denotes the unknown continuous

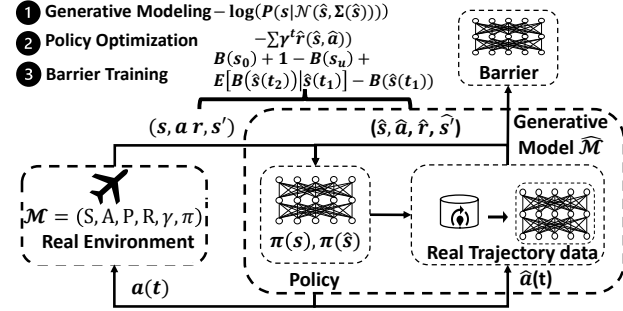


Figure 2: The overview of our safe RL framework based on a generative-model-based soft barrier function. The real environment and generative model share the learning policy and the generative model is abstracted as a discrete-time stochastic differential equation (SDE). We jointly conduct generative modeling, policy optimization, and barrier learning in this framework.

and smooth stochastic environment dynamics without jump condition. The rewards function $r(s, a) : \mathcal{S} \times \mathcal{A} \rightarrow \mathbb{R}$ is known and the discount factor $\gamma \in [0, 1]$. A deterministic continuous NN-based policy $\pi_\theta : \mathcal{S} \rightarrow \mathcal{A}$ maps the states $s(t) \in \mathcal{S}$ to an action $a(t) \in \mathcal{A}$ at time t as $a(t) = \pi_\theta(s(t))$, where $s(t)$ is a random variable at timestep t . The environment has several known spaces, i.e., the state space $\mathcal{S} \subset \mathcal{S}$, the initial space $\mathcal{S}_0 \subset \mathcal{S}$, and the unsafe space $\mathcal{S}_u \subset \mathcal{S}$. The RL objective is to maximize the total discounted expected return as

$$\max_{\theta} J := \mathbb{E}_{s(0) \in \mathcal{S}_0, P(s'|s, a)} \left[\sum_{t=0}^T \gamma^t r(s(t), a(t)) \right], P \in \mathcal{P}.$$

Assumption 3.1. The dynamics of the environment is assumed to be continuous and smooth. Thus, this paper does not consider discontinuous hybrid dynamics such as contact dynamics in Mujoco and Safety Gym. Such an assumption is not uncommon, as it remains a challenging open problem to learn the discontinuous dynamics (Parmar et al., 2021; Pfrommer et al., 2021).

We address the hard safety chance constraint for RL by requiring the control policy with a safety probability lower bound, as defined below.

Definition 3.2. (Safety Probability Lower Bound) A safety probability lower bound $1 - \eta$ of the entire trajectory (process) $\tau_\theta = \{s(0), s(1), \dots, s(T)\}$ is defined as $P(s(t) \notin \mathcal{S}_u | s(0) \in \mathcal{S}_0, \forall t \in [0, T]) \geq 1 - \eta, \eta \in [0, 1]$.

RL with hard safety chance constraints vs. CMDP: Typically, the safe constraints of CMDP are *at the cumulative trajectory cost level* as

$$\max_{\theta} J(\pi_\theta) \text{ s.t. } \mathbb{E} \left[\sum_t \gamma^t c(s(t), a(t)) \right] \leq C,$$

while our safe RL considers more challenging chance constraints (safety probability lower bound) *at the time point level along the entire trajectory as*

$$\max_{\theta} J(\pi_{\theta}),$$

s.t. $P(s(t) \notin S_u | \pi_{\theta}, s(0)) \geq 1 - \eta, \forall t \in [0, T], \forall s(0) \in S_0,$ (1)

where P denotes the safe probability starting from any initial state at any time step.

Definition 3.3. (Bi-level Optimization Problem for Safe RL) To solve the chance-constrained RL in Equation (1), we formulate a bi-level optimization problem for our framework as the following, where we use $\hat{\cdot}$ to denote the elements related to the generative model:

$$\max_{\theta, \alpha} J(\pi_{\theta}) - \lambda \eta^*(\theta, \alpha)^2 - \mathcal{L}_g(\tau_{\theta}, \hat{\tau}_{\theta, \alpha}),$$

where $\eta^*(\theta, \alpha)$ denotes the upper bound of unsafe probability and is the optimal objective to a lower-level problem of the generative-model-based soft barrier function with \hat{s} as the synthetic state in the generative model:

$$\begin{aligned} & \min_{\beta} \eta, \\ \text{s.t. } & \begin{cases} B_{\beta}(\hat{s}) \geq 0, \forall \hat{s} \in S, \\ B_{\beta}(\hat{s}) \geq 1, \forall \hat{s} \in S_u, \\ B_{\beta}(\hat{s}) \leq \eta, \forall \hat{s} \in S_0, \\ \mathbb{E}[B_{\beta}(\hat{s}(t+1)) | \hat{s}(t)] \leq B_{\beta}(\hat{s}(t)), \\ \hat{s}(t+1) = \hat{\mathcal{M}}_{\theta, \alpha}(\hat{s}(t)), \forall t \in [0, T]. \end{cases} \end{aligned} \quad (2)$$

Here θ is the parameter of policy π . α is the parameter of the generative model $\hat{\mathcal{M}}_{\theta, \alpha} = (\hat{G}_{\alpha}, \hat{\Sigma}_{\alpha})$, which is a stochastic differential equation (SDE) with \hat{G}_{α} as the drift function and $\hat{\Sigma}_{\alpha}$ as the diffusion function for the stochasticity, as shown later in Equation (3). $\lambda \geq 0$ is a penalty multiplier. $\tau_{\theta} := \{s(0), s(1), \dots, s(T)\}$ and $\hat{\tau}_{\theta, \alpha} := \{\hat{s}(0), \hat{s}(1), \dots, \hat{s}(T)\}$ are the sampled realizations of stochastic processes (trajectories) from the environment and from the generative model by the policy π_{θ} , respectively. β is the parameter of the generative-model-based soft barrier function $B_{\beta} : \mathbb{R}^n \rightarrow \mathbb{R}^+$. We encode the hard safety chance constraint by the generative-model-based soft barrier function B_{β} in the lower problem, which minimizes $\eta^*(\theta, \alpha)$ as the upper bound of the unsafe probability for $\hat{\mathcal{M}}_{\theta, \alpha}$ in Section 3.3. The upper problem aims to optimize the policy's expected return $J(\pi_{\theta})$ and learn the generative model by the maximum likelihood loss $\mathcal{L}_g(\tau_{\theta}, \hat{\tau}_{\theta, \alpha})$ between the processes τ_{θ} and $\hat{\tau}_{\theta, \alpha}$ as shown later in Equation (4). Moreover, the upper problem penalizes $\eta^*(\theta, \alpha)$, which can back propagate the gradient information through $\hat{\mathcal{M}}_{\theta, \alpha}$ to π_{θ} for pushing the agent to avoid S_u in the MDP \mathcal{M}_{θ} as long as $\hat{\mathcal{M}}_{\theta, \alpha}$ behaves similar to \mathcal{M}_{θ} .

Algorithm 1 Safe RL with the Generative-model-based Soft Barrier Function

Input: Unknown environment \mathcal{M}_{θ} with an initial policy π_{θ}

Output: Policy π_{θ} with soft barrier function B_{β} based on generative model $\hat{\mathcal{M}}_{\theta, \alpha}$

- 1: **for** k in $0, \dots, N$ **do**
- 2: **for** i in $0, \dots, M$ **do**
- 3: Sample processes τ_{θ}^i by policy π_{θ} with \mathcal{M}_{θ} and synthetic processes $\hat{\tau}_{\theta, \alpha}^i$ by π_{θ} with $\hat{\mathcal{M}}_{\theta, \alpha}$.
- 4: Compute generative loss function \mathcal{L}_g with τ_{θ}^i and $\hat{\tau}_{\theta, \alpha}^i$ as in Equation (4), $\alpha \leftarrow \alpha - \frac{\partial \mathcal{L}_g}{\partial \alpha}$.
- 5: **end for**
- 6: Compute barrier function loss \mathcal{L}_B by sampling synthetic $\hat{\tau}_{\theta, \alpha}^k$ as in Equation (5).
- 7: Compute total discount reward $\hat{J}(\pi_{\theta})$ by sampling synthetic $\hat{\tau}_{\theta, \alpha}^k$ as in Equation (6).
- 8: $\theta \leftarrow \theta - \frac{\partial \mathcal{L}_B}{\partial \theta} + \frac{\partial \hat{J}}{\partial \theta}, \beta \leftarrow \beta - \frac{\partial \mathcal{L}_B}{\partial \beta}$.
- 9: **end for**

We can compute the gradient from $\eta^*(\theta, \alpha)$ for π_{θ} through $\hat{\mathcal{M}}_{\theta, \alpha}$ with current auto-differential tools. This cannot be done in \mathcal{M}_{θ} as it is unknown. Therefore, the overall bi-level problem is end-to-end differentiable and can be solved efficiently. Figure 2 shows how the components in our framework interact with each other. The overall algorithm to solve the bi-level problem is shown in Algorithm 1. Next, we are going to introduce the details of each module.

3.2. Generative Modeling

The role of the generative model in our framework is two folds: (1) Because the barrier function requires an environment model to encode the hard safety chance constraints, the generative model serves as a surrogate model to build this barrier function, where $\eta^*(\theta, \alpha)$ propagates the gradient to π_{θ} through $\hat{\mathcal{M}}_{\theta, \alpha}$ for improving system safety. (2) The generative model can generate synthetic process (trajectory) $\hat{\tau}_{\theta, \alpha}$ to optimize the performance of the policy efficiently.

We learn the generative model $\hat{\mathcal{M}}_{\theta, \alpha}$ as a discrete-time SDE to capture the dynamics and stochasticity of the environment and serve as a base for the construction of the soft barrier function:

$$\hat{\mathcal{M}}_{\theta, \alpha} : \hat{s}(t+1) = \hat{G}_{\alpha}(\hat{s}(t), \pi_{\theta}(\hat{s}(t))) + \hat{\Sigma}_{\alpha}(\hat{s}(t))W(t), \quad (3)$$

where $\hat{G}_{\alpha} : \mathbb{R}^n \times \mathbb{R}^m \rightarrow \mathbb{R}^n$ is an unknown drift function, unknown diffusion function $\hat{\Sigma}_{\alpha} : \mathbb{R}^n \rightarrow \mathbb{R}^{n \times d}$ outputs a $n \times d$ matrix based on \hat{s} , and $W(t) \in \mathbb{R}^d$ is the Brownian motion (also known as Wiener Process) with dimension d , encoding the stochasticity. When the environment is deterministic, we can simply set the $\hat{\Sigma}(s)$ as $\mathbf{0}$. We design the generative model to share the learning control policy with

the real environment, as shown in Figure 2. For the inference, the generative model starts from a sample $\hat{s}(0) \in S_0$ and rolls out by drift function \hat{G}_α , diffusion function $\hat{\Sigma}_\alpha$, and policy π_θ . Therefore, the computation graph contains the learning policy; thus, the auto-differential tools can obtain the gradient for the policy by back-propagating through the generative model.

Remark 3.4. We use the fully-connected neural networks to encode such an SDE. Due to the continuity of the neural net, such SDE specification requires the environment dynamics to be continuous and smooth. Therefore our approach cannot handle hybrid dynamics with jump conditions such as the contact dynamics in Mujoco and Safety Gym, as mentioned earlier in Assumption 3.1.

The generative model training is to reduce the following loss function:

$$\begin{aligned} & \min_{\alpha} \mathcal{L}_g(\tau_\theta, \hat{\tau}_{\theta, \alpha}) \\ & = \min_{\alpha} - \sum_{t=0}^T \log \left(P \left(s(t) \mid \mathcal{N}(\hat{s}(t), \hat{\Sigma}_\alpha(\hat{s}(t))) \right) \right), \end{aligned} \quad (4)$$

where \mathcal{L}_g is the maximum likelihood loss, $P \left(s(t) \mid \mathcal{N}(\hat{s}(t), \hat{\Sigma}_\alpha(\hat{s}(t))) \right)$ is the likelihood probability of the observed $s(t)$ under the normal distribution of the SDE representation. We use `torchsde` (Li et al., 2020b) to fit the data $\tau_\theta = \{s(0), s(1), \dots, s(T)\}$ to the generative model by updating its parameter α , which is shown in Lines 2 to 5 in the Algorithm 1.

3.3. Soft Barrier Function Learning

To encode the hard chance constraint, we introduce a novel generative-model-based soft barrier function.

Definition 3.5. (Barrier Function for SDE) Given a policy π_θ , B_β is a generative-model-based soft barrier function for the discrete-time SDE $\hat{\mathcal{M}}_{\theta, \alpha}$ as in Equation (3), if it is twice differentiable and satisfies the constraints of the lower problem in Equation (2).

Lemma 3.6. (Prajna et al., 2004) *Let $B(\hat{s}(t))$ be a supermartingale of the process $\hat{s}(t)$ and $B(\hat{s}) \geq 0, \forall \hat{s} \in S$. Then for any $\hat{s}(0) \in S_0, c > 0, P(\sup_{t \geq 0} B(\hat{s}(t)) \geq c \mid \hat{s}(0) \in S_0) \leq \frac{B(\hat{s}(0))}{c}$.*

Theorem 3.7. *With a barrier function as in Definition 3.5, the generative-model SDE with policy π_θ (Equation (3)) has a safety probability lower bound $1 - \eta^*$, where η^* is the optimal value in the lower problem of Equation (2), as $\forall t \in [0, T], P(\hat{s}(t) \notin S_u \mid \hat{s}(0) \in S_0) \geq 1 - \eta^*, \hat{s}(t+1) = \hat{\mathcal{M}}_{\theta, \alpha}(\hat{s}(t))$.*

Proof: With the last two conditions of the constraints in the lower problem of Equation (2), we have

$$\mathbb{E}[B(\hat{s}(t_2)) \mid \hat{s}(t_1)] \leq B(\hat{s}(t_1)), \forall T \geq t_2 \geq t_1 \geq 0,$$

where $\hat{s}(t_2)$ is the future state of $\hat{s}(t_1)$ by the generative model. This indicates that the barrier function $B(\hat{s})$ is a supermartingale. Then by leveraging the Lemma 1 above from (Prajna et al., 2004), we have

$$\begin{aligned} & P(\hat{s}(t) \in S_u, \text{ for some } t \in [0, T] \mid \hat{s}(0) \in S_0) \\ & \leq P(B(\hat{s}(t)) \geq 1, \text{ for some } t \in [0, T] \mid \hat{s}(0) \in S_0) \\ & \leq P \left(\sup_{t \in [0, T]} B(\hat{s}(t)) \geq 1 \mid \hat{s}(0) \in S_0 \right) \leq B(\hat{s}(0)) \leq \eta^*. \end{aligned}$$

Therefore, the safety probability lower bound is $1 - \eta^*$, and Theorem 3.7 holds. \square

We further translate the constraints of the lower problem in Equation (2) with their sampling mean:

$$\begin{aligned} & \min_{\beta} \eta, \\ \text{s.t.}, & \begin{cases} \frac{1}{N} \sum_{i=1}^N B_\beta(\hat{s}^i(0)) \leq \eta, \hat{s}^i(0) \in S_0, \\ \frac{1}{N} \sum_{i=1}^N B_\beta(\hat{s}_u^i) \geq 1, \hat{s}_u^i \in S_u, \\ \frac{1}{N} \sum_{i=1}^N B_\beta(\hat{s}^i) \geq 0, \hat{s}^i \in S, \\ \frac{1}{N} \sum_{i=1}^N B_\beta(\hat{s}^i(t+1)) \leq B_\beta(\hat{s}^i(t)), \\ \hat{s}^i(t+1) = \hat{\mathcal{M}}_{\theta, \alpha}(\hat{s}^i(t)), t \in [0, T]. \end{cases} \end{aligned}$$

The third non-negative condition is easy to satisfy by setting the output activation function as *Sigmoid* for the barrier neural network. The last two conditions are to make B as a supermartingale, which is the key to deriving the lower bound of safety probability for the trajectory. In practice, we use a supervised-learning-based method to optimize this problem by minimizing the following loss function:

$$\begin{aligned} \min_{\theta, \beta} \mathcal{L}_B & = \frac{1}{N} \sum_{i=1}^N B_\beta(\hat{s}^i(0)) + \frac{1}{N} \sum_{i=1}^N (1 - B_\beta(\hat{s}_u^i)) \\ & + \frac{1}{N} \sum_{i=1}^N \left(\frac{1}{M} \sum_{j=1}^M B_\beta(\hat{s}^{i,j}(t+1)) - B_\beta(\hat{s}^i(t)) \right), \\ & \hat{s}^{i,j}(t+1) = \hat{\mathcal{M}}_{\theta, \alpha}(\hat{s}^i(t)), t \in [0, T], \end{aligned} \quad (5)$$

where $\hat{s}^{i,j}(t+1)$ is the next state of $\hat{s}^i(t)$ sampled from the generative model $\hat{\mathcal{M}}_{\theta, \alpha}$ with policy π_θ . \mathcal{L}_B essentially reduces the barrier mapping value on S_0 (the maximum is $\eta^*(\theta, \alpha)$) and projects the unsafe space S_u to 1 with *Sigmoid* output, and decreases the expectation of the barrier function along with trajectory. It is worth noting that \mathcal{L}_B cannot be approximated by the real environment \mathcal{M}_θ with policy π_θ , as we cannot sample from any intermediate time point $s(t)$ to $s(t+1)$ to compute the last sample mean in Equation (5), which is relatively feasible and simple to do with $\hat{\mathcal{M}}_{\theta, \alpha}$ as in Equation (3). The barrier training can be terminated if the second and third sample means in Equation (5) are zero and non-positive, respectively. The soft barrier training is shown as Line 6 in Algorithm 1.

3.4. Policy Optimization

As stated before, we use the generative model to generate synthetic data $\hat{\tau}_{\theta, \alpha}^i = \{\hat{s}^i(0), \dots, \hat{s}^i(T)\}$ ($i \in [1, N]$) with policy π_θ to maximize the total expected return $\hat{J}(\pi_\theta)$ as:

$$\begin{aligned} \max_{\pi_\theta} \hat{J}(\pi_\theta) &= \mathbb{E}_{\hat{s}(0), \hat{\mathcal{M}}_{\theta, \alpha}} \left[\sum_{t=0}^T \gamma^t r(\hat{s}(t), \pi_\theta(\hat{s}(t))) \right] \\ \text{s.t. } \hat{s}(t+1) &= \hat{\mathcal{M}}_{\theta, \alpha}(\hat{s}(t)), \forall t \in [0, T]. \end{aligned}$$

We use the sample mean from the synthetic trajectories as an estimate for the expectation:

$$\begin{aligned} \max_{\pi_\theta} \hat{J}(\pi_\theta) &= \frac{1}{N} \sum_{i=0}^N \sum_{t=0}^T \gamma^t r(\hat{s}^i(t), \pi_\theta(\hat{s}^i(t))), \quad (6) \\ \text{s.t. } \hat{s}^i(t+1) &= \hat{\mathcal{M}}_{\theta, \alpha}(\hat{s}^i(t)), \forall t \in [0, T]. \end{aligned}$$

With policy π_θ in the computation graph of $\hat{\mathcal{M}}_{\theta, \alpha}$, we can directly obtain the backwards gradient for π_θ from Equation (6). The policy optimization is shown as Line 7 in the Algorithm 1.

3.5. Theoretical Analysis of Safety Probability under Soft Barrier

For the *final learned* policy, we conduct a theoretical analysis of its safety probability (as defined in Definition 3.2), derived from the generative-model-based soft barrier function in our framework.

Lemma 3.8. (Theorem 21 in (Agarwal et al., 2020a)) Given $\delta \in (0, 1)$, a learned deterministic policy $\pi_\theta(s)$ and assume the environment-policy transition dynamics as $P^*(s'|s) \in \mathcal{P}$ with the function class $|\mathcal{P}| < \infty$ (s' represents the next state of s), let the environment and policy generate a dataset of n trajectories $D := \{(s^j(t), s^j(t+1))\}_{t=0}^T$ ($j = 1, \dots, n$), $s(t) \sim D^t = (s^j(0:t-1))$. Note that D^t is a martingale depending on the previous examples. Let the generative model $\hat{\mathcal{M}}_{\theta, \alpha}$ maximize the likelihood of the dataset by its transition dynamics \hat{P} via Equation (4). Then with at least probability $1 - \delta$, the expectation of total variation distance between P^* and \hat{P} is bounded as:

$$\begin{aligned} &\sum_{t=0}^T \mathbb{E}_{s \sim D^t} \left[d_{\text{TV}}(P^*, \hat{P}) \right] \\ &= \sum_{t=0}^T \mathbb{E}_{s \sim D^t} \left\| \hat{P}(s'|s) - P^*(s'|s) \right\|_{\text{TV}}^2 \leq \frac{2 \log(|\mathcal{P}|/\delta)}{n}. \end{aligned} \quad (7)$$

Lemma 3.9. Given a random variable $X_n \geq 0$ on a probability space Ω , if $\mathbb{E}_\Omega[X_n] \rightarrow 0$ as $n \rightarrow \infty$, then $P(X_n = 0) \rightarrow 1$.

Proof: For any $m \in \mathbb{N}$, let $E_m = \{\omega \in \Omega : X_n(\omega) > \frac{1}{m}\}$.

Since $X_n \geq 0$, we have:

$$\mathbb{E}_\Omega[X_n] = \int_\Omega X_n dP \geq \int_{E_m} X_n dP \geq \frac{1}{m} P(E_m).$$

Therefore, $P(E_m) \rightarrow 0$, and then:

$$\begin{aligned} 0 \leq P(\{\omega \in \Omega : X_n(\omega) \neq 0\}) &= P(\bigcup E_m) \\ &= \lim_{m \rightarrow \infty} P(E_m) \rightarrow 0, \end{aligned}$$

$$\begin{aligned} P(\{\omega \in \Omega : X_n(\omega) \neq 0\}) &\rightarrow 0 \\ \implies P(\{\omega \in \Omega : X_n(\omega) = 0\}) &\rightarrow 1. \end{aligned}$$

Proposition 3.10. (Asymptotic Lower Bound of Safety Probability) Given the learned policy π_θ , let the generative model fit n sample trajectories τ_θ^i ($i = 1, \dots, n$) from environment \mathcal{M}_θ with π_θ by Equation (4), learn the generative-model-based soft barrier function B_β by Equation (5) with η^* and assume that it formally satisfies the constraints in Equation (2), then the real environment \mathcal{M}_θ with policy π_θ is safe with probability at least $(1 - \eta^*)$ when $n \rightarrow \infty$.

Proof of Proposition 3.10: Given (S, \mathcal{B}) as the measure spaces with S as the state space and $\mathcal{B} = \{B : S \rightarrow \mathbb{R}, \|B\|_\infty \leq 1\}$, where B is a generative-model-based soft barrier function with *Sigmoid* output, then according to the definition of total variation distance and Lemma 3.8, we can bound the expectation of the difference between the barrier values of the real trajectory and the synthetic trajectory as

$$\begin{aligned} &\sum_{t=0}^T \mathbb{E}_{s \sim D^t} \left[\frac{1}{2} \sup_{B \in \mathcal{B}} \mathbb{E}_{P^*(s'|s)}[B(s')] - \mathbb{E}_{\hat{P}(s'|s)}[B(s')] \right] \\ &= \sum_{t=0}^T \mathbb{E}_{s \sim D^t} \left[d_{\text{TV}}(P^*, \hat{P}) \right] \leq \frac{2 \log(|\mathcal{P}|/\delta)}{n}. \end{aligned}$$

When $n \rightarrow \infty$, we set $\delta = \frac{1}{n}$ and let $X_n = \frac{1}{2} \sup_{B \in \mathcal{B}} \mathbb{E}_{P^*(s'|s)}[B(s')] - \mathbb{E}_{\hat{P}(s'|s)}[B(s')]$, and therefore $\mathbb{E}[X_n] \rightarrow 0$. We know $X_n \geq 0$, since $X_n = 0$ when $P^* = \hat{P}$. Therefore, according to Lemma 3.9, $P(X_n \rightarrow 0) \rightarrow 1$. We then assume D^t ($t \in [0, T]$) can uniformly cover the space S as $n \rightarrow \infty$, thus the soft barrier becomes a true barrier function for the real environment and Proposition 3.10 holds. \square

Remark 3.11. (Practical Safety Probability Lower Bound) In addition to the asymptotic safety probability, we propose a finite-sample practical safety probability lower bound. We first sample the generative model and the environment with the final learned policy to quantify their maximum distance per state as $\Delta = \max_{t \in [0, T], i=1, \dots, N} |s^i(t) - \hat{s}^i(t)|$, and then enlarge the unsafe region with Δ by Minkowski sum as $S'_u = S_u \oplus \Delta$. Next, we retrain another generative-model-based soft barrier function B with S'_u . Finally, we conservatively report

$(1 - \max_{(\hat{s} \in \hat{\mathcal{S}}_t^i, i=1, \dots, N)} B(\hat{s}_t^i))$ as the final lower bound of safety probability by the soft barrier function.

Remark 3.12. (During-learning Safety) The above asymptotic and practical safety bounds are derived for the final learned policy. It is possible that $1 - \eta^*$ is not a valid safety probability bound during learning, as there exists a modeling gap between the generative model and the real environment. However, we optimize $1 - \eta^*$ during learning to increase the chance of finding safer learned policies at the end, as demonstrated in our experiments below.

4. Experimental Results

Experiment Settings and Examples: As stated in Section 2, other model-based safe RL methods with hard safety constraints either require known dynamics, a safe initial/backup policy, or human intervention, and thus do not apply to the problem setting we are considering. Therefore, we compare our approach with two state-of-the-art open-source model-free CMDP-based methods, PPO-L (Ray et al., 2019) and FOCOPS (Zhang et al., 2020). For these two baselines, we design the cost function such that the state is safe if its cost is less than 0. It is worth noting that PPO-L has a stronger safety constraint than FOCOPS as we implemented the PPO-L with the expectation of cost per state as $\mathbb{E}[c(s, a)] \leq 0$, rather than the cumulative cost in FOCOPS as $\mathbb{E}[\sum_{t=0}^T c(s, a) \leq D']$. In FOCOPS, We conservatively set $D' = -60$ for the 2D and cartpole examples below, and -200 for the Rocket and UAV examples, to improve its safety. We mark this safety-oriented version as FOCOPS*. We mainly compare the converged final policy of each method in system safe rate measured via simulations – we call it *empirical safe rate*. We also perform safety probability analysis for our method (CMDP cannot provide one), and compare different methods in total reward return.

Note that learning safe control policy for high-dimensional systems under hard safety constraints is quite challenging. Current state-of-the-art works of certificate-based policy learning mainly focus on low-dimensional systems with fewer than 9D states (Luo & Ma, 2021; Lindemann et al., 2021; Chang et al., 2019; Berkenkamp et al., 2017; Dawson et al., 2022). In this paper, among the four examples shown below, we are able to test our approach on 13D UAV and Rocket examples:

2-Dimensional SDE (Prajna et al., 2004) has the unknown dynamics \mathcal{M} as $s_1 = 0.8s_2, ds_2 = (a - 0.3s_1^3)dt + 0.2dW(t)$ ($W(t)$, Wiener process.) Initial space $S_0 = \{(s_1 + 2)^2 + s_2 \leq 0.01\}$, and unsafe space $S_u = \{s_1 \in [-1, 0], s_2 \in [1.2, 1.7]\}$. The goal is to stabilize the system near $(0, 0)$.

Cartpole Balancing has a 4-dimensional vector $s =$

$[x, \theta, \dot{x}, \dot{\theta}]$ as the system state, where x is the position and θ is the angular error to the upright. The initial space $S_0 = \{(x, \theta, \dot{x}, \dot{\theta}) | x \in [-0.167, 0.033], \theta \in [-0.6, -0.5], \dot{x} = -0.35, \dot{\theta} = 0.53\}$, and unsafe space $S_u = \{(x, \theta, \dot{x}, \dot{\theta}) | x \leq -0.75\}$. The goal is to keep the cartpole balanced upright.

Powered Rocket Landing (Jin et al., 2021) has 6 DoF (degrees of freedom) with 13 system states and 3 action variables. The goal is to land the rocket close to the original point while avoiding an unsafe region. Its state vector is $\mathbf{s} = [\mathbf{p} \ \mathbf{v} \ \mathbf{q} \ \omega] \in \mathbb{R}^{13}$, where $\mathbf{p} = (x, y, z) \in \mathbb{R}^3$ and $\mathbf{v} = (v_x, v_y, v_z) \in \mathbb{R}^3$ represent the position and velocity of the rocket, respectively. $\mathbf{q} \in \mathbb{R}^4$ is the unit quaternion for attitude and $\omega \in \mathbb{R}^3$ is the angular velocity with respect to the inertial frame. There are three thrust forces for the rocket as the control input $\mathbf{u} = [T_x, T_y, T_z] \in \mathbb{R}^3$. Initial space $S_0 : \mathbf{p} = (x, y, z)(x - 10)^2 + (y + 8)^2 + (z - 5)^2 \leq 0.01, \mathbf{v} = 0, \mathbf{q} = (0.73, 0, 0, 0.68), \omega = 0$, and unsafe space $S_u : \mathbf{p} = (x, y, z)(x - 5)^2 + y^2 \leq 1, -2 \leq z \leq 5, \|\mathbf{v}\|_1 \leq 10, \|\omega\|_1 \leq 10$.

UAV Maneuvering (Jin et al., 2021) is to maneuver a UAV close to the original point while avoiding an obstacle. The 6-DoF UAV has 13 system states and 4 action variables. Its state vector is $\mathbf{s} = [\mathbf{p} \ \mathbf{v} \ \mathbf{q} \ \omega] \in \mathbb{R}^{13}$, same with above Rocket example. The control input $\mathbf{u} = [T_1, T_2, T_3, T_4] \in \mathbb{R}^4$ includes the four rotating propellers of the quadrotor. Initial space $S_0 : \mathbf{p} = (x, y, z)(x + 8)^2 + (y + 6)^2 + (z - 9)^2 \leq 0.01, \mathbf{v} = 0, \mathbf{q} = (1, 0, 0, 0), \omega = 0$, unsafe space $S_u : \mathbf{p} = (x, y, z)(x + 4.5)^2 + (y + 4)^2 \leq 1, -2 \leq z \leq 5$.

Comparison and Effectiveness of Our Approach: Table 1 shows the comparison results in simulation-based system safe rate (based on 500 simulations for each example, with random initial states), safety probability, and performance for 5 individual runs. We can see that **by directly enforcing hard safety constraints via soft barrier functions, our approach can achieve significantly higher system safe rates than the CMDP-based baselines. Our approach also provides a practical lower bound of safety probability, which the CMDP-based methods cannot provide.** CMDP achieves better performance (total reward return) in some cases, but we view safety as the first priority for these systems and the focus of this work.

Figure 3 shows the control trajectories by the learned policies from our approach and the baselines. The agent is safe with our learned policy, while there exist unsafe cases by both PPO-L and FOCOPS. Moreover, our generative model behaves very similarly to the real environment, which shows the usefulness of the generative modeling for constructing the soft barrier function and optimizing the control policy. We also show the learning process of the soft barrier function on the generative model and its testing in the real environment in Figures 4-7 for all the examples. The learned

Table 1: Comparison of our approach with CMDP-based baselines PPO-L and FOCOPS*. s_e is the safe rate by simulating 500 random initial states from S_0 . $1 - \eta$ is the practical lower bound of safety probability in our approach as $(1 - \max_{(\hat{s} \in \hat{\tau}_t^i, i=1, \dots, n)} B(\hat{s}_t^i))$, derived by **Remark 3.11**. We report the mean and std values (in parenthesis) for 5 individual runs. Our approach achieves significantly higher s_e than the baselines. It is observed that $1 - \eta$ is a lower bound of s_e .

Metric	Methods	2D	Cartpole	Rocket	UAV
s_e , empirical safe rate	Ours	99.9(0.09)%	100%	100%	100%
	PPO-L	98.9(0.08)%	89.3(5.5)%	96.4(6.3)%	100%
	FOCOPS*	98.7(0.18)%	84.2(4)%	100%	91(4.2)%
$1 - \eta$, safety lower bound	Ours	97.6(1.3)%	86.6(2.9)%	89.9(1.6)%	93.2(2.2)%
	PPO-L, FOCOPS*	-	-	-	-
$J(\pi)$, performance	Ours	-67.3(4.9)	-24.4(4.7)	-143.2(1.6)	-847.1(6.5)
	PPO-L	-66.3(5.3)	-34.1(6.7)	-151.4(3.6)	-895.5(4.3)
	FOCOPS*	-69.8(3.2)	-15.2(2.3)	-249.1(1.4)	-734.1(3.3)

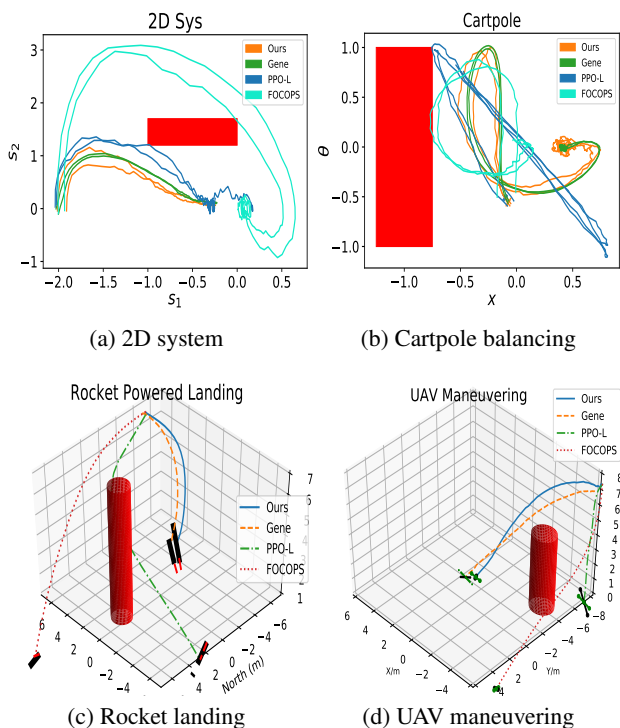


Figure 3: Control trajectories by the learned policies from our approaches and baselines. “Gene” indicates the synthetic trajectory from the final learned generative model, which behaves very similarly to the real environment with the “Ours” policy, showing its effectiveness for barrier function construction. We can see that our approach learns safer policies than the baselines.

barrier function maps the initial space to near 0 and the unsafe space to 1 with the third sample mean in Equation (5) to 0 (marked as Lie in Figures). The barrier function has a

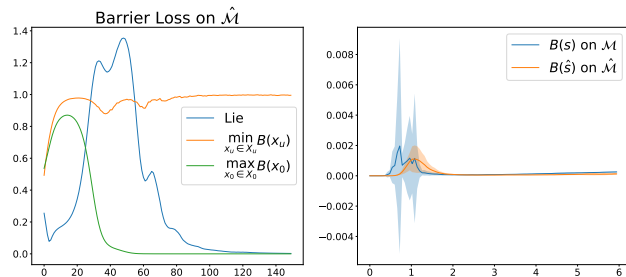


Figure 4: Barrier function training and testing in the 2D SDE example. The learned barrier function maps the initial space to near 0 and the unsafe space to 1 with the third sample mean in Equation (5) to 0 (marked as Lie). The barrier function has a similar close-to-0 value keeping constant along with the trajectories in the real environment and the generative model.

similar value along with the trajectories in the real environment and the generative model. Again, this indicates that the generative model behaves very similarly to the environment, as shown in Figure 3. Although the barrier function decreases or stays constant most of the time, it can increase at some point. This is due to 1) the possible modeling error between the generative model SDE and environment and 2) the supervised learning approach cannot cover all possible cases for soft barrier function training.

Limitations: As stated earlier, one key assumption of this work is the smoothness and continuity of the system behavior, which prevents its application to hybrid dynamics with jump conditions such as the contact dynamics in Mujoco and Safety Gym. One possible solution is to learn an ensemble generative model as a hybrid system to deal with those discontinuous contact dynamics, and we plan to explore it in future work. Another limitation of our framework is the computation complexity of the generative model (e.g.,

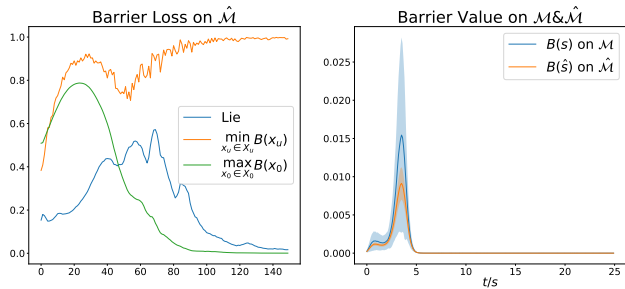


Figure 5: Barrier function training and testing in the Cartpole balancing example.

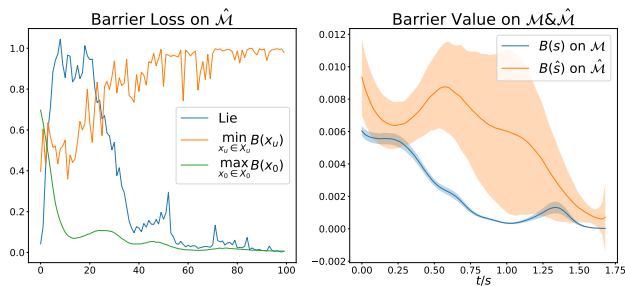


Figure 6: Barrier function training and testing in the UAV maneuvering example.

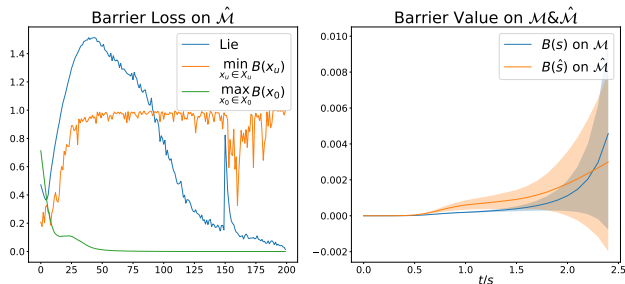


Figure 7: Barrier function training and testing in the Rocket powered landing example.

it takes around 8 hours to learn a policy for the Cartpole example and 1 day for the UAV and Rocket examples). In future work, we plan to improve the efficiency of this part by exploring techniques such as Continuous Latent Process Flows (CLPF) (Deng et al., 2021).

5. Conclusion

We present a safe RL approach in unknown continuous stochastic environments that enforces hard reachability-based safety constraints through generative-model-based soft barrier functions. Our approach formulates a novel bi-level optimization problem and develops a safety RL algorithm that jointly learns the generative model, soft barrier function, and policy optimization. Experiments demonstrate that our approach can significantly improve empirical system safe rates over CMDP-based baselines and also provide a practical lower bound of safety probability.

Acknowledgements

We gratefully acknowledge funding support by National Science Foundation (NSF) grants 1834701, 1724341, 2038853, Department of Energy (DOE) award DE-EE0009150, and Office of Naval Research grant N00014-19-1-2496.

References

Agarwal, A., Kakade, S., Krishnamurthy, A., and Sun, W. Flambe: Structural complexity and representation learning of low rank mdps. *Advances in neural information processing systems*, 33:20095–20107, 2020a.

Agarwal, A., Kakade, S., and Yang, L. F. Model-based reinforcement learning with a generative model is minimax optimal. In *Conference on Learning Theory*, pp. 67–83. PMLR, 2020b.

Altman, E. *Constrained Markov decision processes: stochastic modeling*. Routledge, 1999.

Ames, A. D., Xu, X., Grizzle, J. W., and Tabuada, P. Control barrier function based quadratic programs for safety critical systems. *IEEE Transactions on Automatic Control*, 62(8):3861–3876, 2016.

As, Y., Usmanova, I., Curi, S., and Krause, A. Constrained policy optimization via bayesian world models. In *International Conference on Learning Representations*, 2021.

Bai, Q., Bedi, A. S., Agarwal, M., Koppel, A., and Agarwal, V. Achieving zero constraint violation for constrained reinforcement learning via primal-dual approach. In *Proceedings of the AAAI Conference on Artificial Intelligence*, volume 36, pp. 3682–3689, 2022.

- 495 Bastani, O., Li, S., and Xu, A. Safe reinforcement learning
 496 via statistical model predictive shielding. In *Robotics:
 497 Science and Systems*, 2021.
 498
- 499 Berkenkamp, F., Turchetta, M., Schoellig, A., and Krause,
 500 A. Safe model-based reinforcement learning with stability
 501 guarantees. *Advances in neural information processing
 502 systems*, 30, 2017.
 503
- 504 Bharadhwaj, H., Kumar, A., Rhinehart, N., Levine, S.,
 505 Shkurti, F., and Garg, A. Conservative safety critics
 506 for exploration. In *International Conference on Learning
 507 Representations*.
- 508 Chang, Y.-C., Roohi, N., and Gao, S. Neural lyapunov control.
 509 *Advances in neural information processing systems*,
 510 32, 2019.
 511
- 512 Cheng, R., Orosz, G., Murray, R. M., and Burdick, J. W.
 513 End-to-end safe reinforcement learning through barrier
 514 functions for safety-critical continuous control tasks. In
 515 *Proceedings of the AAAI Conference on Artificial Intelli-
 516 gence*, volume 33, pp. 3387–3395, 2019.
 517
- 518 Choi, J., Castaneda, F., Tomlin, C. J., and Sreenath, K. Rein-
 519 forcement learning for safety-critical control under model
 520 uncertainty, using control lyapunov functions and control
 521 barrier functions. *arXiv preprint arXiv:2004.07584*,
 522 2020.
 523
- 524 Chow, Y., Ghavamzadeh, M., Janson, L., and Pavone, M.
 525 Risk-constrained reinforcement learning with percentile
 526 risk criteria. *The Journal of Machine Learning Research*,
 527 18(1):6070–6120, 2017.
- 528 Chow, Y., Nachum, O., Duenez-Guzman, E., and
 529 Ghavamzadeh, M. A lyapunov-based approach to safe
 530 reinforcement learning. *Advances in neural information
 531 processing systems*, 31, 2018.
 532
- 533 Dalal, G., Dvijotham, K., Vecerik, M., Hester, T., Paduraru,
 534 C., and Tassa, Y. Safe exploration in continuous action
 535 spaces. *arXiv preprint arXiv:1801.08757*, 2018.
 536
- 537 Dawson, C., Qin, Z., Gao, S., and Fan, C. Safe nonlinear
 538 control using robust neural lyapunov-barrier functions. In
 539 *Conference on Robot Learning*, pp. 1724–1735. PMLR,
 540 2022.
 541
- 542 Deng, R., Brubaker, M. A., Mori, G., and Lehrmann, A.
 543 Continuous latent process flows. *Advances in Neural
 544 Information Processing Systems*, 34:5162–5173, 2021.
- 545 Ding, D., Wei, X., Yang, Z., Wang, Z., and Jovanovic, M.
 546 Provably efficient safe exploration via primal-dual policy
 547 optimization. In *International Conference on Artificial
 548 Intelligence and Statistics*, pp. 3304–3312. PMLR, 2021.
 549
- Emam, Y., Glotfelter, P., Kira, Z., and Egerstedt, M. Safe
 model-based reinforcement learning using robust control
 barrier functions. *arXiv preprint arXiv:2110.05415*, 2021.
- Fan, J., Huang, C., Chen, X., Li, W., and Zhu, Q. Reachnn*:
 A tool for reachability analysis of neural-network controlled
 systems. In Hung, D. V. and Sokolsky, O. (eds.),
Automated Technology for Verification and Analysis, pp.
 537–542, Cham, 2020. Springer International Publishing.
 ISBN 978-3-030-59152-6.
- HasanzadeZonuzy, A., Bura, A., Kalathil, D., and Shakkotai,
 S. Learning with safety constraints: Sample complex-
 ity of reinforcement learning for constrained mdps. In
*Proceedings of the AAAI Conference on Artificial Intelli-
 gence*, volume 35, pp. 7667–7674, 2021.
- Huang, C., Fan, J., Li, W., Chen, X., and Zhu, Q. Reachnn:
 Reachability analysis of neural-network controlled sys-
 tems. *ACM Transactions on Embedded Computing Sys-
 tems (TECS)*, 18(5s):1–22, 2019.
- Huang, C., Xu, S., Wang, Z., Lan, S., Li, W., and Zhu, Q.
 Opportunistic intermittent control with safety guarantees
 for autonomous systems. *Design Automation Conference
 (DAC’20)*, 2020.
- Huang, C., Fan, J., Chen, X., Li, W., and Zhu, Q. Polar:
 A polynomial arithmetic framework for verifying neural-
 network controlled systems. In *Automated Technology
 for Verification and Analysis*. Springer International Pub-
 lishing, 2022.
- Jin, W., Mou, S., and Pappas, G. J. Safe pontryagin differ-
 entiable programming. *Advances in Neural Information
 Processing Systems*, 34:16034–16050, 2021.
- Li, G., Wei, Y., Chi, Y., Gu, Y., and Chen, Y. Breaking
 the sample size barrier in model-based reinforcement
 learning with a generative model. *Advances in neural
 information processing systems*, 33:12861–12872, 2020a.
- Li, X., Wong, T.-K. L., Chen, R. T. Q., and Duvenaud, D.
 Scalable gradients for stochastic differential equations.
*International Conference on Artificial Intelligence and
 Statistics*, 2020b.
- Lindemann, L., Hu, H., Robey, A., Zhang, H., Dimarogonas,
 D., Tu, S., and Matni, N. Learning hybrid control barrier
 functions from data. In *Conference on Robot Learning*,
 pp. 1351–1370. PMLR, 2021.
- Liu, X., Huang, C., Wang, Y., Zheng, B., and Zhu, Q.
 Physics-aware safety-assured design of hierarchical neu-
 ral network based planner. In *2022 ACM/IEEE 13th Inter-
 national Conference on Cyber-Physical Systems (ICCPs)*,
 pp. 137–146. IEEE, 2022.

- 550 Liu, X., Jiao, R., Wang, Y., Han, Y., Zheng, B., and Zhu,
551 Q. Safety-assured speculative planning with adaptive
552 prediction. 2023a.
- 553 Liu, X., Jiao, R., Zheng, B., Liang, D., and Zhu, Q. Safety-
554 driven interactive planning for neural network-based lane
555 changing. In *Proceedings of the 28th Asia and South
556 Pacific Design Automation Conference*, pp. 39–45, 2023b.
- 557 Luo, Y. and Ma, T. Learning barrier certificates: Towards
558 safe reinforcement learning with zero training-time vi-
559 olations. *Advances in Neural Information Processing
560 Systems*, 34:25621–25632, 2021.
- 561 Ma, H., Chen, J., Eben, S., Lin, Z., Guan, Y., Ren, Y.,
562 and Zheng, S. Model-based constrained reinforcement
563 learning using generalized control barrier function. In
564 *2021 IEEE/RSJ International Conference on Intelligent
565 Robots and Systems (IROS)*, pp. 4552–4559. IEEE, 2021.
- 566 Maeda, S.-i., Watahiki, H., Ouyang, Y., Okada, S., Koyama,
567 M., and Nagarajan, P. Reconnaissance for reinforcement
568 learning with safety constraints. In *Joint European Con-
569 ference on Machine Learning and Knowledge Discovery
570 in Databases*, pp. 567–582. Springer, 2021.
- 571 Moldovan, T. M. and Abbeel, P. Safe exploration in markov
572 decision processes. *arXiv preprint arXiv:1205.4810*,
573 2012.
- 574 Parmar, M., Halm, M., and Posa, M. Fundamental chal-
575 lenges in deep learning for stiff contact dynamics. In
576 *2021 IEEE/RSJ International Conference on Intelligent
577 Robots and Systems (IROS)*, pp. 5181–5188. IEEE, 2021.
- 578 Pfrommer, S., Halm, M., and Posa, M. Contactnets: Learn-
579 ing discontinuous contact dynamics with smooth, implicit
580 representations. In *Conference on Robot Learning*, pp.
581 2279–2291. PMLR, 2021.
- 582 Prajna, S. and Jadbabaie, A. Safety verification of hybrid
583 systems using barrier certificates. In *International Work-
584 shop on Hybrid Systems: Computation and Control*, pp.
585 477–492. Springer, 2004.
- 586 Prajna, S., Jadbabaie, A., and Pappas, G. J. Stochastic safety
587 verification using barrier certificates. In *2004 43rd IEEE
588 conference on decision and control (CDC)(IEEE Cat. No.
589 04CH37601)*, volume 1, pp. 929–934. IEEE, 2004.
- 590 Qin, Z., Zhang, K., Chen, Y., Chen, J., and Fan, C. Learning
591 safe multi-agent control with decentralized neural barrier
592 certificates. *arXiv preprint arXiv:2101.05436*, 2021.
- 593 Ray, A., Achiam, J., and Amodei, D. Benchmarking safe ex-
594 ploration in deep reinforcement learning. *arXiv preprint
595 arXiv:1910.01708*, 7:1, 2019.
- 596 Shao, Y. S., Chen, C., Kousik, S., and Vasudevan, R.
597 Reachability-based trajectory safeguard (rts): A safe and
598 fast reinforcement learning safety layer for continuous
599 control. *IEEE Robotics and Automation Letters*, 6(2):
600 3663–3670, 2021.
- 601 Shen, L., Yang, L., Chen, S., Yuan, B., Wang, X., Tao,
602 D., et al. Penalized proximal policy optimization for safe
603 reinforcement learning. *arXiv preprint arXiv:2205.11814*,
604 2022.
- 605 Silver, D., Hubert, T., Schrittwieser, J., Antonoglou, I., Lai,
606 M., Guez, A., Lanctot, M., Sifre, L., Kumaran, D., Grae-
607 pel, T., et al. A general reinforcement learning algorithm
608 that masters chess, shogi, and go through self-play. *Sci-
609 ence*, 362(6419):1140–1144, 2018.
- 610 Stooke, A., Achiam, J., and Abbeel, P. Responsive safety
611 in reinforcement learning by pid lagrangian methods. In
612 *International Conference on Machine Learning*, pp. 9133–
613 9143. PMLR, 2020.
- 614 Taylor, A., Singletary, A., Yue, Y., and Ames, A. Learning
615 for safety-critical control with control barrier functions.
616 In *Learning for Dynamics and Control*, pp. 708–717.
617 PMLR, 2020.
- 618 Tirinzoni, A., Poiani, R., and Restelli, M. Sequential transfer
619 in reinforcement learning with a generative model. In
620 *International Conference on Machine Learning*, pp. 9481–
621 9492. PMLR, 2020.
- 622 Turchetta, M., Berkenkamp, F., and Krause, A. Safe explo-
623 ration in finite markov decision processes with gaussian
624 processes. *Advances in Neural Information Processing
625 Systems*, 29, 2016.
- 626 Wachi, A., Sui, Y., Yue, Y., and Ono, M. Safe exploration
627 and optimization of constrained mdps using gaussian
628 processes. In *Proceedings of the AAAI Conference on
629 Artificial Intelligence*, volume 32, 2018.
- 630 Wagener, N. C., Boots, B., and Cheng, C.-A. Safe rein-
631 forcement learning using advantage-based intervention.
632 In *International Conference on Machine Learning*, pp.
633 10630–10640. PMLR, 2021.
- 634 Wang, Y., Huang, C., and Zhu, Q. Energy-efficient control
635 adaptation with safety guarantees for learning-enabled
636 cyber-physical systems. In *Proceedings of the 39th Inter-
637 national Conference on Computer-Aided Design*, pp. 1–9,
638 2020.
- 639 Wang, Y., Huang, C., Wang, Z., Xu, S., Wang, Z., and
640 Zhu, Q. Cocktail: Learn a better neural network con-
641 troller from multiple experts via adaptive mixing and
642 robust distillation. In *58th ACM/IEEE Design Automa-
643 tion Conference, DAC 2021, San Francisco, CA, USA*,

- December 5-9, 2021, pp. 397–402. IEEE, 2021a. doi: 10.1109/DAC18074.2021.9586148. URL <https://doi.org/10.1109/DAC18074.2021.9586148>.
- Wang, Y., Huang, C., Wang, Z., Wang, Z., and Zhu, Q. Design-while-verify: Correct-by-construction control learning with verification in the loop. In *59th ACM/IEEE Design Automation Conference, DAC 2022, San Francisco, CA, USA, July 10-14, 2022*, 2022.
- Wang, Y., Zhan, S., Wang, Z., Huang, C., Wang, Z., Yang, Z., and Zhu, Q. Joint differentiable optimization and verification for certified reinforcement learning. *International Conference on Cyber-Physical Systems*, 2023.
- Wang, Z., Huang, C., Kim, H., Li, W., and Zhu, Q. Cross-layer adaptation with safety-assured proactive task job skipping. *ACM Trans. Embed. Comput. Syst.*, 20(5s), sep 2021b. ISSN 1539-9087. doi: 10.1145/3477031. URL <https://doi.org/10.1145/3477031>.
- Wang, Z., Liang, H., Huang, C., and Zhu, Q. Cross-layer design of automotive systems. *IEEE Design Test*, 38(5): 8–16, 2021c. doi: 10.1109/MDAT.2020.3037561.
- Wei, T., Wang, Y., and Zhu, Q. Deep reinforcement learning for building hvac control. In *2017 54th ACM/EDAC/IEEE Design Automation Conference (DAC)*, pp. 1–6, June 2017. doi: 10.1145/3061639.3062224.
- Xu, S., Fu, Y., Wang, Y., O’Neill, Z., and Zhu, Q. Learning-based framework for sensor fault-tolerant building hvac control with model-assisted learning. In *Proceedings of the 8th ACM International Conference on Systems for Energy-Efficient Buildings, Cities, and Transportation, BuildSys ’21*, pp. 1–10, New York, NY, USA, 2021a. Association for Computing Machinery. ISBN 9781450391146. doi: 10.1145/3486611.3486644. URL <https://doi.org/10.1145/3486611.3486644>.
- Xu, S., Fu, Y., Wang, Y., Yang, Z., O’Neill, Z., Wang, Z., and Zhu, Q. Accelerate online reinforcement learning for building hvac control with heterogeneous expert guidances. In *Proceedings of the 9th ACM International Conference on Systems for Energy-Efficient Buildings, Cities, and Transportation, BuildSys ’22*, pp. 89–98, New York, NY, USA, 2022. Association for Computing Machinery. ISBN 9781450398909. doi: 10.1145/3563357.3564064. URL <https://doi.org/10.1145/3563357.3564064>.
- Xu, T., Liang, Y., and Lan, G. Crpo: A new approach for safe reinforcement learning with convergence guarantee. In *International Conference on Machine Learning*, pp. 11480–11491. PMLR, 2021b.
- Yang, L., Huang, B., Li, Q., Tsai, Y.-Y., Lee, W. W., Song, C., and Pan, J. Tacgmn: Learning tactile-based in-hand manipulation with a blind robot using hierarchical graph neural network. *IEEE Robotics and Automation Letters*, 8(6):3605–3612, 2023.
- Yang, Q., Simão, T. D., Tindemans, S. H., and Spaan, M. T. Wcsac: Worst-case soft actor critic for safety-constrained reinforcement learning. In *Proceedings of the AAAI Conference on Artificial Intelligence*, volume 35, pp. 10639–10646, 2021.
- Yang, Z., Huang, C., Chen, X., Lin, W., and Liu, Z. A linear programming relaxation based approach for generating barrier certificates of hybrid systems. In *International Symposium on Formal Methods*, pp. 721–738. Springer, 2016.
- Yu, D., Ma, H., Li, S., and Chen, J. Reachability constrained reinforcement learning. In *International Conference on Machine Learning*, pp. 25636–25655. PMLR, 2022.
- Zhang, Y., Vuong, Q., and Ross, K. First order constrained optimization in policy space. *Advances in Neural Information Processing Systems*, 33:15338–15349, 2020.
- Zhao, W., Queraltá, J. P., and Westerlund, T. Sim-to-real transfer in deep reinforcement learning for robotics: a survey. In *2020 IEEE Symposium Series on Computational Intelligence (SSCI)*, pp. 737–744. IEEE, 2020.
- Zhu, Q., Li, W., Kim, H., Xiang, Y., Wardega, K., Wang, Z., Wang, Y., Liang, H., Huang, C., Fan, J., and Choi, H. Know the unknowns: Addressing disturbances and uncertainties in autonomous systems. In *Proceedings of the 39th International Conference on Computer-Aided Design, ICCAD ’20, New York, NY, USA, 2020*. Association for Computing Machinery. ISBN 9781450380263. doi: 10.1145/3400302.3415768. URL <https://doi.org/10.1145/3400302.3415768>.
- Zhu, Q., Huang, C., Jiao, R., Lan, S., Liang, H., Liu, X., Wang, Y., Wang, Z., and Xu, S. Safety-assured design and adaptation of learning-enabled autonomous systems. In *Proceedings of the 26th Asia and South Pacific Design Automation Conference, ASPDAC ’21*, pp. 753–760, New York, NY, USA, 2021. Association for Computing Machinery. ISBN 9781450379991. doi: 10.1145/3394885.3431623. URL <https://doi.org/10.1145/3394885.3431623>.